SCIENTIFIC REPORTS

OPEN

SUBJECT AREAS:
TECHNICAL REPORT
CORTEX
AUTISM SPECTRUM DISORDERS
SYNAPTIC DEVELOPMENT

Received
15 April 2013

Accepted
4 September 2013

Published
9 October 2013

Correspondence and requests for materials should be addressed to K.M. (kamila.markram@epfl.ch)

Nlgn4 knockout induces network hypo-excitability in juvenile mouse somatosensory cortex *in vitro*

V. Delattre, D. La Mendola, J. Meystre, H. Markram & K. Markram

Laboratory of Neural Microcircuitry, Brain Mind Institute, Ecole Polytechnique Fédérale de Lausanne, Switzerland.

Neuroligins (Nlgns) are postsynaptic cell adhesion molecules that form transynaptic complexes with presynaptic neurexins and regulate synapse maturation and plasticity. We studied the impact of the loss of Nlgn4 on the excitatory and inhibitory circuits in somatosensory cortical slices of juvenile mice by electrically stimulating these circuits using a multi-electrode array and recording the synaptic input to single neurons using the patch-clamp technique. We detected a decreased network response to stimulation in both excitatory and inhibitory circuits of Nlgn4 knock-out animals as compared to wild-type controls, and a decreased excitation-inhibition ratio. These data indicate that Nlgn4 is involved in the regulation of excitatory and inhibitory circuits and contributes to a balanced circuit response to stimulation.

Neuroligins 1–4 (Nlgn1–4), which are widely expressed in the rodent central nervous system[1–3], are crucial postsynaptic adhesion proteins that contribute to synaptic organization and function[2–5]. It has been reported in *in vivo* studies that each Neuroligin isoform localizes primarily to a specific synapse subpopulation: Nlgn1 to glutamatergic, Nlgn2 to GABAergic and Nlgn3 to both GABAergic and glutamatergic synapses[1,6–9]. Nlgn4 is present in glycinergic post synaptic structures in many areas of the central nervous system, including the retina, thalamus, colliculi, brainstem and the spinal cord[10], and the absence of Nlgn4 in the retina results in a decreased number of glycine receptors and corresponding alterations of glycinergic currents[10].

To determine the function of Nlgn4 at the level of a network such as the cortical column, we used acute somatosensory cortex slices, network stimulation with three dimensional multi-electrode arrays (3D-MEAs) and single cell patch-clamp recordings of layer 2/3 pyramidal cells to capture the network activity. The effects of electrical stimulation of the entire network surrounding the recorded cell were compared between Nlgn4 knock-out (KO) and wild-type (WT) littermates. By clamping the cell at different membrane potentials, we could separately measure excitatory and inhibitory driving forces triggered by the network electrical stimulation[11]. We observed a decreased network response to stimulation in both excitatory and inhibitory circuits of Nlgn4-KO mice as well as a striking frequency-dependent effect of the Nlgn4-KO on the delay to the peak network response and on the paired-pulsed ratio. In addition, we report changes in the expression levels of selected synaptic proteins in Nlgn4-KO brain that may correlate with possible circuit rewiring due to the loss of Nlgn4.

Results

Decreased excitation. Individual neurons were recorded in voltage-clamp mode at a voltage of −60 mV to measure the contribution of excitatory inputs and stimulated via the MEA at different stimulus frequencies (Figure 1A). When comparing average measures for network excitability between WT (n = 12) and Nlgn4-KO (n = 15) animals (Table 1), we found that the total excitatory charge triggered by MEA stimulation was reduced in Nlgn4 KOs for all tested frequencies, and that the peak current was significantly decreased in Nlgn4 KOs for all tested frequencies except for the 100 Hz stimulation (Table 1). The relative decrease in the charge and the peak currents in Nlgn4 KOs were inversely proportional to the stimulation frequency, ranging from an approximately 70% decrease at low stimulation frequencies to a 40% decrease at high stimulation frequencies. Moreover, the time to peak was significantly increased in Nlgn4 KOs at 5, 10, 50, 75 and 100 Hz stimulation frequencies (Figure 1B and Table 1). In the cases of 75 and 100 Hz stimulations, the network response in WT built up until it reached a maximum around 70 ms (75 Hz) and 150 ms (100 Hz) and then decreased, whereas in Nlgn4 KOs the network response built up continuously (Figure 1B). Scaling and overlaying the averaged waveforms revealed no differences between WT and Nlgn4 KO in the rise and decay kinetics of individual excitatory

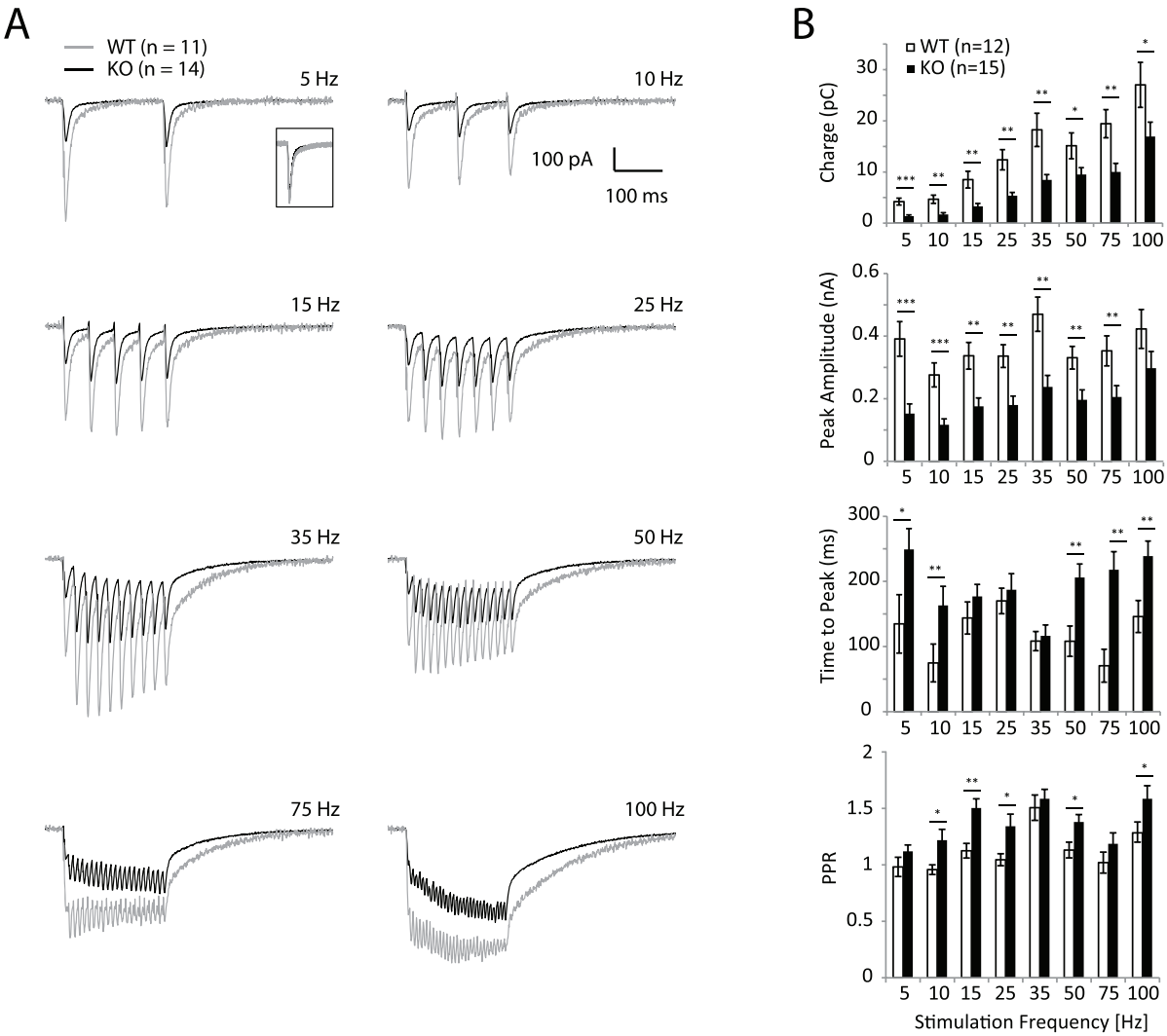

Figure 1 | **Excitatory Components of Network Response.** (A): Averaged network response to frequency stimulation recorded in L2/3 pyramidal cell in voltage-clamp mode (V = −60 mV) WT: 12 cells (grey), KO: 15 cells (black), each cell response is an average of 5 repetitions. Inset: scaled and overlaid averaged waveforms. (B): Network response properties (top to bottom): total charge, peak response amplitude, time to peak, and paired-pulse ratio (PPR).

Table 1 | Impact of NLGN4-KO on excitatory circuits

Frequency (Hz)		5	10	15	25	35	50	75	100
Charge (pC)	WT	4.3 ± 0.7	4.7 ± 0.9	8.6 ± 1.8	12.4 ± 2.2	18.3 ± 3.6	15.3 ± 2.7	19.5 ± 3.0	26.8 ± 4.8
	KO	1.4 ± 0.3	1.7 ± 0.4	3.3 ± 0.6	5.4 ± 0.7	8.4 ± 1.1	9.5 ± 1.4	10.2 ± 1.8	17.1 ± 3.0
	t-value	4.5	3.7	3.4	3.7	3.2	2.3	3.1	2.1
	p-value	*** **$1.e^{-4}$**	** **$1.e^{-3}$**	** **$2.e^{-3}$**	** **$1.e^{-3}$**	** **$3.e^{-3}$**	* **$2.e^{-2}$**	** **$5.e^{-3}$**	* **0.04**
Peak (nA)	WT	0.40 ± 0.06	0.28 ± 0.04	0.34 ± 0.05	0.34 ± 0.04	0.47 ± 0.06	0.33 ± 0.04	0.36 ± 0.05	0.42 ± 0.07
	KO	0.15 ± 0.03	0.11 ± 0.02	0.17 ± 0.03	0.18 ± 0.03	0.24 ± 0.04	0.2 ± 0.03	0.2 ± 0.04	0.3 ± 0.06
	t-value	4.2	4.1	3.5	3.5	3.7	2.8	2.6	1.7
	p-value	*** **$3.e^{-4}$**	***$4.e^{-4}$**	** **$2.e^{-3}$**	** **$1.e^{-3}$**	** **$1.e^{-3}$**	** **$4.e^{-3}$**	** **$8.e^{-3}$**	0.09
Latency (ms)	WT	118 ± 46	66 ± 30	142 ± 26	170 ± 21	98 ± 12	111 ± 25	73 ± 27	142 ± 27
	KO	245 ± 34	173 ± 29	178 ± 20	189 ± 26	119 ± 18	203 ± 22	217 ± 30	236 ± 24
	t-value	2.6	2.8	1.5	1.1	1.3	3.0	3.7	2.9
	p-value	* **0.02**	** **$9.e^{-3}$**	0.14	0.30	0.19	** **$5.e^{-3}$**	** **$1.e^{-4}$**	** **$8.e^{-3}$**
PPR	WT	0.96 ± 0.09	0.97 ± 0.04	1.14 ± 0.06	1.04 ± 0.06	1.51 ± 0.11	1.16 ± 0.07	1.02 ± 0.04	1.29 ± 0.10
	KO	1.09 ± 0.10	1.22 ± 0.09	1.51 ± 0.09	1.36 ± 0.09	1.59 ± 0.08	1.38 ± 0.08	1.18 ± 0.16	1.61 ± 0.12
	t-value	1.7	2.5	3.3	3.0	1.1	2.3	1.3	2.2
	p-value	0.10	* **$1.e^{-2}$**	** **$3.e^{-3}$**	** **$6.e^{-3}$**	0.27	* **$2.e^{-2}$**	0.20	* **$3.e^{-2}$**

postsynaptic currents[12] (inset Figure 1A). The paired-pulse ratios (PPR) measured as the ratio between the responses following the 1st and the 2nd pulse during train stimulation, were significantly increased at 10, 15, 25, 50 and 100 Hz stimulation frequencies in Nlgn4 KOs (Table 1), indicating a distinct synaptic facilitation that could be a consequence of Nlgn4 KO or represent a compensatory mechanism (Figure 1B). Taken together, our findings show that the overall excitatory response at the network level is smaller and slower in Nlgn4 KO animals, indicating decreased network excitability when compared to WT controls.

Decreased inhibition. Individual neurons were recorded in voltage-clamp mode at a voltage of +10 mV to measure the contribution of inhibitory inputs and stimulated via the MEA at different stimulus frequencies (Figure 2A). In Nlgn4 KOs, the total inhibitory charge and peak current were significantly decreased for all frequencies at and below 50 Hz (Table 2). Both the charge and the peak current were decreased in Nlgn4 KOs in a manner that was inversely proportional to the stimulation frequency, with a relative decrease ranging from approximately 55% at low frequencies to 15% at high frequencies. The time to peak was increased significantly for 75 and 100 Hz stimulation frequencies (Table 2). In the cases of 75 and 100 Hz stimulations, the network response in WT built up until it reached a maximum around 50 ms (75 Hz) or 100 ms (100 Hz) and then decreased. On the contrary, the network response in Nlgn4 KOs built up and then plateaued (Figure 2B). As with excitatory responses, scaling and overlaying the averaged waveforms revealed no differences in the rise and decay kinetics of individual inhibitory postsynaptic currents[12] (inset Figure 2A). The PPR was significantly increased at 25 Hz stimulation, indicating a facilitation of the inhibitory response at this particular stimulation rate. In summary, the network inhibitory response in Nlgn4 KOs is smaller, and slower for very high stimulation frequencies (Figure 2B).

Decreased excitation to inhibition ratio. Overall, the charge ratio of excitation vs. inhibition was significantly decreased in Nlgn4 KO mice ($t = 4.60$, $p = 7.e^{-6}$, Figure 3A). When analyzed in more detail over the different stimulation frequencies, this decrease was significant for 75 Hz ($t = 2.35$, $p = 0.02$) and 100 Hz stimulations ($t = 2.17$, $p = 0.03$), whereas for all other tested frequencies, a non-significant trend towards a decrease of the excitation-inhibition ratio was observed (Figure 3B).

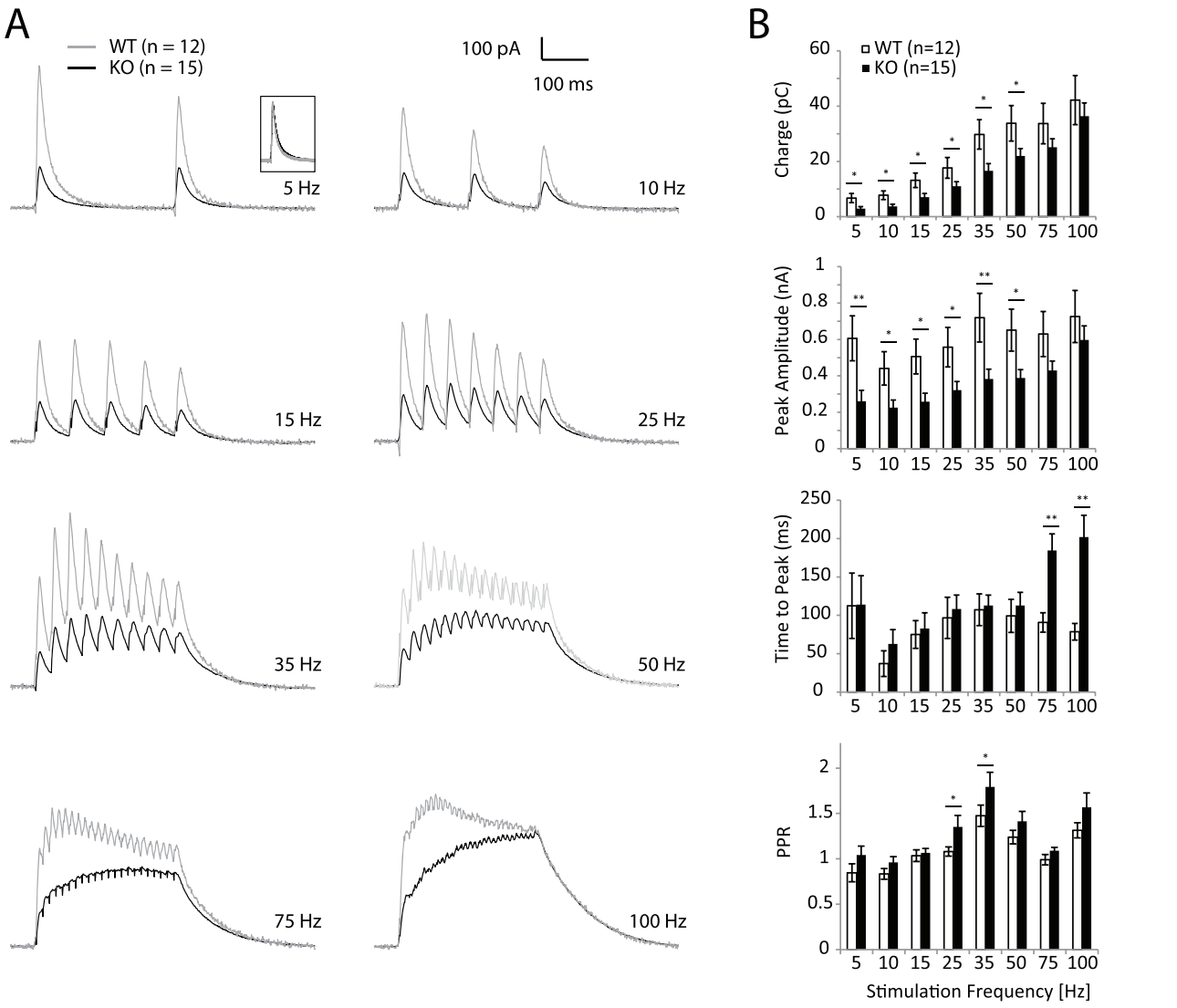

Figure 2 | Inhibitory Components of Network Response. (A): Averaged network response to frequency stimulation recorded in L2/3 pyramidal cell in voltage-clamp mode (V = +10 mV). WT: 12 cells (grey), KO: 15 cells (black), each cell response is an average of 5 repetitions. Inset: scaled and overlaid averaged waveforms. (B): Network response properties (top to bottom): total charge, peak response amplitude, time to peak, and paired-pulse ratio (PPR).

Table 2 | Impact of NLGN4-KO on inhibitory circuits

Frequency (Hz)		5	10	15	25	35	50	75	100
Charge (pC)	WT	7.2 ± 1.7	8.0 ± 1.7	13.6 ± 2.8	18.1 ± 3.5	29.8 ± 4.1	34.3 ± 5.8	34.1 ± 8.0	42.5 ± 9.7
	KO	2.9 ± 0.7	3.7 ± 0.8	6.9 ± 1.4	11.0 ± 1.8	16.6 ± 2.7	21.5 ± 2.8	24.6 ± 3.2	36.4 ± 4.8
	t-value	2.8	2.7	2.5	2.1	2.7	2.2	1.6	1.2
	p-value	* **1.e^{-2}**	* **1.e^{-2}**	* **1.e^{-2}**	* **4.e^{-2}**	* **1.e^{-2}**	* **4.e^{-2}**	0.12	0.22
Peak (nA)	WT	0.63 ± 0.13	0.45 ± 0.10	0.52 ± 0.10	0.57 ± 0.12	0.74 ± 0.14	0.66 ± 0.13	0.63 ± 0.13	0.72 ± 0.16
	KO	0.26 ± 0.06	0.23 ± 0.04	0.26 ± 0.05	0.33 ± 0.05	0.38 ± 0.06	0.38 ± 0.05	0.42 ± 0.05	0.60 ± 0.08
	t-value	3.0	2.6	2.8	2.4	2.8	2.5	2.0	1.4
	p-value	** **6.e^{-3}**	* **1.e^{-2}**	* **1.e^{-2}**	* **2.e^{-2}**	** **9.e^{-3}**	* **1.e^{-2}**	0.06	0.17
Latency (ms)	WT	94 ± 42	39 ± 18	74 ± 20	95 ± 29	97 ± 20	101 ± 23	89 ± 14	77 ± 11
	KO	99 ± 37	55 ± 18	77 ± 21	97 ± 15	105 ± 12	108 ± 18	181 ± 23	195 ± 29
	t-value	0.7	1.1	0.7	0.7	0.9	0.9	3.5	3.7
	p-value	0.46	0.27	0.46	0.47	0.37	0.39	** **1.e^{-3}**	** **1.e^{-3}**
PPR	WT	0.87 ± 0.10	0.84 ± 0.06	1.04 ± 0.07	1.08 ± 0.06	1.49 ± 0.13	1.27 ± 0.08	1.06 ± 0.06	1.31 ± 0.09
	KO	1.10 ± 0.11	0.98 ± 0.07	1.09 ± 0.05	1.38 ± 0.13	1.87 ± 0.15	1.49 ± 0.10	1.27 ± 0.11	1.64 ± 0.16
	t-value	1.9	1.8	1.2	2.2	2.2	2.0	2.0	2.0
	p-value	0.07	0.08	0.25	* **3.e^{-2}**	* **4.e^{-2}**	0.06	0.06	0.05

Protein expression. Gene knockouts can potentially cause changes in the expression of many other proteins and an exhaustive study of every possible compensatory or reactionary response to the constitutive loss of Nlgn4 was not in the scope of this study. Our data however suggested that the effect of the Nlgn4 KO was stronger on excitatory than on inhibitory circuits, resulting in a network hypo-excitability. We therefore tested for changes in the expression of N-methyl-D-aspartate receptor (NMDAR) subunits and the metabotropic glutamate receptor 5 (mGluR-5) that are important for determining synaptic efficacy and mediating circuit re-wiring[13,14]. We used Western blot analysis to quantify relative expression levels of the NMDAR subunits NR1, NR2a, NR2b, and mGluR5 (Figure 4) and found a significant up-regulation of NR1 ($t = 3.12$, $p = 9.e^{-3}$) and mGluR5 levels ($t = 2.31$, $p = 0.04$) in Nlgn4 KO brain, but no significant changes in NR2a and NR2b expression. Since these changes would counter the loss of synaptic function we assume they are part of a compensatory reaction to the KO.

Neuroligins are cell adhesion molecules (CAM), we therefore tested if the constitutive loss of Nlgn4 affected other cell adhesion molecules. We selected the neural cell adhesion molecule (NCAM) and its variant attached with polysialic acid (PSA-NCAM) that operate through different mechanisms from those of the neuroligins. Both NCAM ($t = 8.77$, $p = 3.e^{-6}$) and PSA-NCAM levels ($t = 5.59$, $p = 2.e^{-4}$) were significantly over-expressed in Nlgn4-KO mice as compared to the wild-types, which also appears to be a compensatory response.

Discussion

We observed that the absence of Nlgn4 significantly affects the microcircuits in the S1 region of the juvenile mouse cortex. Both excitatory and inhibitory components of the network response to MEA stimulation were decreased in Nlgn4-KO mice as compared

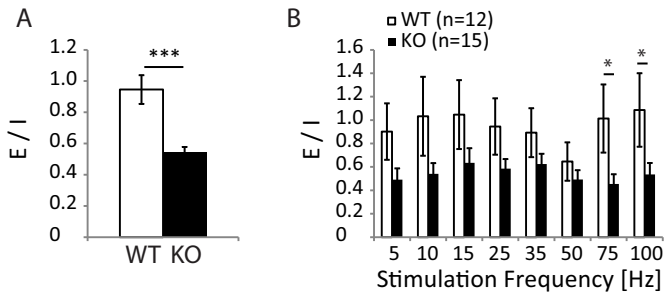

Figure 3 | Network Excitatory Inhibitory Balance. (A): Global excitatory – inhibitory ratio. (B): Frequency-dependent response.

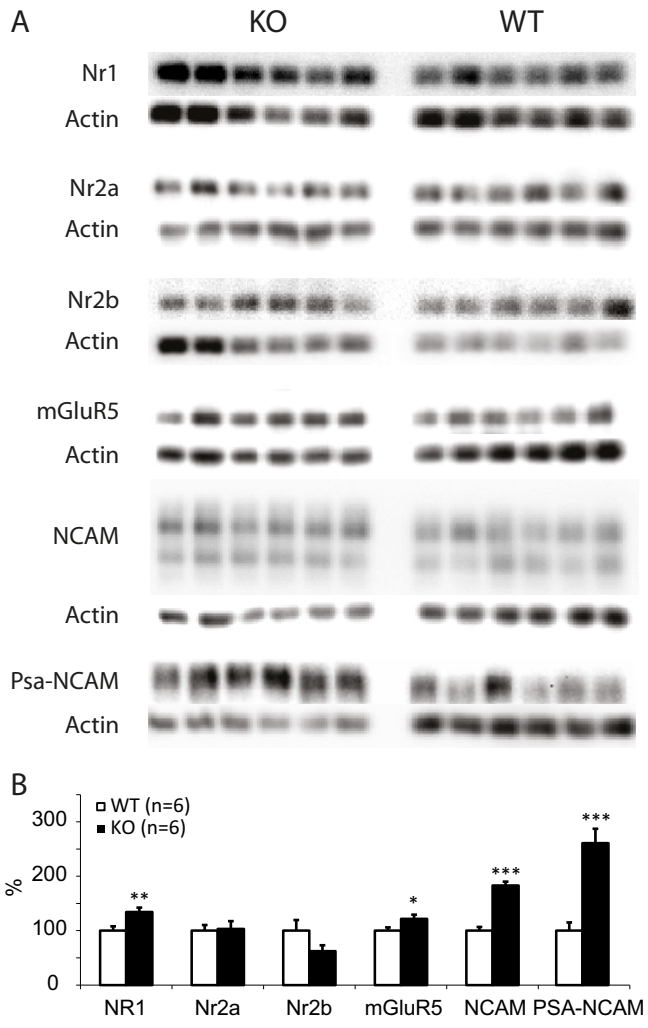

Figure 4 | Nlgn4-KO Impact on Chosen Synaptic Proteins. (A): Western-Blot for each synaptic protein and its respective actin control. Western-Blot images were cropped for comparaison. KO and WT were run on the same gel, actin controls were run on a separated gel in identical conditions. Full-length gels are presented in Supplementary Figure 1. (B): Western-Blot data is normalized to averaged WT expression.

to WT controls. These findings suggest that Nlgn4 is present at both excitatory and inhibitory postsynapses, an observation that has also been made for Nlgn3[15], the closest neuroligin isoform of Nlgn4[16], and probably its ancestor gene[17]. Since the decrease in the excitatory component of the network response in Nlgn4-KOs was greater than in the inhibitory component, the loss of Nlgn4 results in a hypo-excitable network.

We did not observe any differences in the rise and decay kinetics of individual postsynaptic currents, but the latency of maximum network response of both excitatory and inhibitory circuits is slower for many tested stimulation frequencies. In particular at high stimulation frequencies, the network response builds-up and saturates in Nlgn4-KO animals whereas it decays after reaching a maximum in WT controls. This might be explained by a decrease in synaptic release probability[18] in Nlgn4-KO animals, but would require further experimental testing. A decreased of both excitatory and inhibitory conductance accompanied with an increased response latency of projections to layer 2/3 pyramidal cells in the somato-sensory cortex has been observed in sensory-deprived animals[19]. Despite no difference in footpad sensitivity has been reported in adults animals[3], it remains a possibility that Nlgn4-KO juvenile mice have less sensitive footpads.

An increase in PPR indicates an increase in pre-synaptic calcium concentration, and frequency dependent increase in the PPR implies frequency dependent calcium accumulation. Complex calcium mechanisms have been reported to occur within very narrow frequency ranges (10–20 Hz wide) such as calcium electrogenesis in distal dendrites[20]. Therefore, such a frequency dependent calcium accumulation is physiologically possible given the high variety of calcium channels in the pre-synaptic terminal. Calcium channels in the pre-synaptic terminal cluster very specifically to neurexins[21] which in turn form complexes with neuroligins. Thus, our data suggest that NLGN4 modulates the pre-synaptic calcium channel population through its interaction with neuroxins and consequently regulates the fine tuning of frequency dependent calcium accumulation. Loss of NLGN4 in the KO mice was seen to result in frequency dependent increase in the PPR, owing to perturbations in the type and density of the pre-synaptic calcium channels, as seen exclusively in the 25–35 Hz frequency range in inhibitory synapses, and at almost all frequencies except at 35 Hz in excitatory synapses.

Nlgn4 loss leads to the overexpression of NR1 and mGluR5 which are involved in synaptic transmission and plasticity, as well as excitatory circuit rewiring[14,22]. NR1 overexpression would be predicted to cause a higher excitatory component of the network response in Nlgn4-KOs, but we observed the opposite. This result would be compatible with a role of Nlgn4 in NMDAR subunit NR1 trafficking and/or docking at the postsynaptic density. NCAM and PSA-NCAM are also overexpressed in NLGN4-KOs, which may reflect a compensatory mechanism of synapse consolidation. It is known that NCAM modulates synaptic long-term potentiation[23] and that PSA-NCAM is required for both the induction of long-term potentiation and depression[24]. Consequently, our observations predict possible alterations of synaptic plasticity mechanisms in Nlgn4 KOs. However, no change in learning and memory abilities of Nlgn4-KO adult animals has been observed[3]. Finally, Nlgn4-KO results in the overexpression of several synaptic proteins, which is not sufficient to restore entirely normal network functionality, demonstrating the importance and the specificity of Nlgn4 function.

The presence of loss-of-function mutations in Nlgn4 in a small number of autistic patients indicates a causal link between Nlgn4 and heritable autism spectrum conditions (ASCs)[17,25]. Moreover, Nlgn4-KO mice exhibit very specific deficits in reciprocal social interactions and communication, reminiscent of ASCs in humans[3]. Therefore the Nlgn4-KO mouse has been proposed as an animal model for autism[3,17,26]. In particular, an increased in EI ratio in neural circuits of multiple ASC animal models has been reported[27,28], including the retina of Nlgn4-KO animals[10]. Thus, the balance between excitation and inhibition is believed to play a major role in the neurobiology of autism[27–29]. However, we found an overall decrease of the EI ratio in the somatosensory cortex and a generally hypo-reactive network. It should however be noted that the change in EI ratio *per se* may be a more important observation than the direction of the change, as shifts in EI ratios are highly variable across brain regions[28], due to different brain functions, microcircuitry layouts and possibly Neuroligin expression[3]. Finally, the valproic acid (VPA) animal model of autism exhibits hyper and not hypo-reactive circuits as found in the Nlgn4 KO mice[11,30]. The Nlgn4-KO animal model of autism therefore implies a major loss of synaptic function while the VPA animal model of autism implies a major increase in synaptic function[31].

Methods

Animals. Mice with a loss-of-function mutation in the murine NLGN4 ortholog Nlgn4[3] were received from Prof. N. Brose (Max Planck Institute for Experimental Medicin, Göttingen, Germany) and were bred at the EPFL animal facility. All animal experimentation was conducted conform the Swiss National Institutional Guidelines on Animal Experimentation and approved by the Swiss Cantonal Veterinary Office Committee for Animal Experimentation. For this study, 4 KO and 2 WT male mice were used for electrophysiological experiments and 6 of each genotype for the Western Blots.

Acute slice preparation. On postnatal days (P) 13 – P15 WT and Nlgn4-KO male mice were rapidly decapitated without anesthesia. 300 μm thick sagittal brain slices were cut in iced artificial cerebrospinal fluid (ACSF) containing (in mM) 125 NaCl, 2.5 KCl, 25 D-glucose, 25 $NaHCO_3$, 1.25 NaH_2PO_4, 2 $CaCl_2$, and 1 $MgCl_2$; all chemicals from Sigma-Aldrich, St. Louis, MO or Merck, Darmstadt, Germany) using a HR2 vibratome (Sigmann Elektronik, Heidelberg, Germany). The primary somatosensory cortex was manually dissected and isolated to obtain rectangular slices of 5–7 mm width and containing the neocortex in its entire height. Optimal slices, with apical cell dendrites running parallel to the slice surface, were selected for recordings. Slices were incubated at 22°C for 30–60 min until mounting in the recording chamber (32–35°C).

Electrophysiological recording. Slices were mounted on a 3D-MEA with 60 pyramidal platinum electrodes (electrode basis: 40 × 40 μm, electrode height: 50–70 μm, electrode interspace: 200 μm; Qwane Bioscience SA, Lausanne, Switzerland) after evaporation of a mounting solution of 0.14 mg/L nitrocellulose in an ethanol (99%) – methanol (1%) mixture. Cells were visualized by infrared differential interference contrast video microscopy using a camera (VX 55, Till Photonics, Gräfelfing, Germany) mounted on an upright microscope (BX 51WI, Olympus, FI, Japan) fitted with a 40 × objective (LUMPLAN, Olympus). Whole-cell recordings were performed using Axopatch 200B amplifiers (Molecular Devices, Union City, CA, USA). Data acquisition, sampled at 5–10 kHz, was performed via an ITC-18 board (Instrutech Co, Port Washington, NY, USA), connected to a computer running IgorPro (Wavemetrics, Portland, OR, USA). The voltage signal was filtered with a 2 kHz Bessel filter. Patch pipettes were pulled with a P-97 Flaming/Brown micropipette puller (Sutter Instruments Co, Novato, CA, USA) and had an initial resistance of 8–10 MΩ. They were filled with standard intracellular solution (ICS) containing (in mM): 110 K-gluconate, 10 KCl, 4 ATP-Mg, 10 phosphocreatine, 0.3 GTP, 10 N-2-hydroxyethylpiperazine-N'-2-ethanesulfonic acid (pH 7.3), and 0.5% biocytin. Neurons were recorded in layer 2/3 in either current-clamp mode (to record voltages) or voltage clamp mode (to record currents). In voltage-clamp experiments, 10 μM QX-314 was added to the intracellular solution for measurement of GABA receptor–mediated currents at +10 mV. Recordings were not corrected for the liquid junction potential between ACSF and ICS (−14 mV). Recorded cells typically had a ≤ 20 MΩ access resistance. The EI ratio was computed as the ratio of excitatory to inhibitory charges, themselves obtained by the integration of the measured currents from the network response triggered by electrical stimulation.

Electrical stimulation. Multi-site extracellular electrical stimulation (1.0–1.5 V biphasic pulses, 1 ms duration for each polarity) was applied via the MEA with a stimulator STG2008 (Multi Channel System, Reutlingen, Germany) to the entire network surrounding the patched cell, simultaneously using the 16 neighboring extra-cellular electrodes (figure 1). We used a 1 Hz train of single pulses with randomly varying amplitude between 1.0 and 2.0 V for calibration. Patched cells were current-clamped, and the stimulation strength was set to half the amplitude triggering the maximum response. The network stimulus consisted of a series of train pulses (300 ms; 5, 10, 15, 25, 35, 50, 75, and 100 Hz) applied in a pseudo-random order (5, 35, 15, 100, 25, 50, 10, and 75 Hz) with a 2 s inter-stimulus interval. Each stimulus series was repeated 5 times at each clamping potential for each cell. To measure the PPR, we computed the ratio between the responses following the 1st and the 2nd pulse during train stimulation. The mean stimulation amplitude was equivalent for the two groups (1.11 V ± 0.04 and 1.16 V ± 0.04 for WT and KO respectively, p-value = 0.22).

Western blot. The somatosensory cortex was micro-dissected and sonicated in 1% SDS buffer. Protein concentrations were quantified with the Lowry method and samples were diluted with distilled water and 1/3 Blue Loading Buffer to a final concentration of 1 μg/μl and subsequently heated at 95°C for 5 minutes while shaking at 600 rpm. Ten μg of each sample was loaded onto a 10% poly-acrylamide gel. Separation was performed at 100 mV for 15 min and at 175 mV for 50 min. Proteins were transferred onto a 0.45 μm membrane at 100 mV for an hour. The membrane was subsequently blocked in 5% skimmed milk in TBS-T for an hour, incubated overnight with the primary antibodies [anti-NR1 (1 : 2000)[32], anti-NR2a (1 : 1000)[33], anti-NR2b (1 : 1000)[32], anti-mGluR5 (1 : 1000)[34], anti-NCAM (1 : 5000)[35], anti-PSA-NCAM (1 : 1000)[36], anti-actin (1 : 5000)[37] and washed for 3 × 10 min with TBS-T. Finally, the membrane was incubated for an hour with the secondary antibody diluted in milk [(anti-mouse (1 : 5000), anti-rabbit 1 : 5000, anti-mouse (1 : 5000), anti-rabbit (1 : 2000), anti-rabbit (1 : 10000), anti-mouse (1 : 2000), anti-mouse (1 : 10000)] washed 3 × 10 min with TBS-T and revealed using ECL.

Equipment and settings. Immunocomplexes were visualized using a chemiluminescence peroxidase substrate (SuperSignal West Dura Extended Duration Substrate, PIERCE). The immunoreactivity was detected using the ChemiDoc XRS system (Bio-Rad Laboratories). For the densitometrical analysis of the bands, Quantity One 4.6.3 software (Bio-Rad Laboratories AG, Switzerland) was used. The values are represented as adjusted volumes, normalized to actin.

Statistics. Experimental data analysis was entirely performed in Matlab (The MathWorks, Inc., Natick, MA, USA) with custom scripts. Data are presented as the mean ± SEM. Paired Student's *t*-tests were applied as statistical tests, and statistical significance was asserted for: $p < 0.05$ (*); $p < 0.01$ (**) and $p < 0.001$ (***).

1. Varoqueaux, F., Jamain, S. & Brose, N. Neuroligin 2 is exclusively localized to inhibitory synapses. *Eur. J. Cell Biol.* **83**, 449–456 (2004).
2. Varoqueaux, F. *et al.* Neuroligins determine synapse maturation and function. *Neuron* **51**, 741–754 (2006).
3. Jamain, S. *et al.* Reduced social interaction and ultrasonic communication in a mouse model of monogenic heritable autism. *Proc. Natl. Acad. Sci. U. S. A.* **105**, 1710–1715 (2008).
4. Ichtchenko, K. *et al.* Neuroligin 1: a splice site-specific ligand for beta-neurexins. *Cell* **81**, 435–443 (1995).
5. Ichtchenko, K., Nguyen, T. & Südhof, T. C. Structures, alternative splicing, and neurexin binding of multiple neuroligins. *J. Biol. Chem.* **271**, 2676–2682 (1996).
6. Chubykin, A. A. *et al.* Activity-dependent validation of excitatory versus inhibitory synapses by neuroligin-1 versus neuroligin-2. *Neuron* **54**, 919–931 (2007).
7. Song, J. Y., Ichtchenko, K., Südhof, T. C. & Brose, N. Neuroligin 1 is a postsynaptic cell-adhesion molecule of excitatory synapses. *Proc. Natl. Acad. Sci. U. S. A.* **96**, 1100–1105 (1999).
8. Hoon, M. *et al.* Neuroligin 2 controls the maturation of GABAergic synapses and information processing in the retina. *J. Neurosci. Off. J. Soc. Neurosci.* **29**, 8039–8050 (2009).
9. Baudouin, S. J. *et al.* Shared synaptic pathophysiology in syndromic and nonsyndromic rodent models of autism. *Science* **338**, 128–132 (2012).
10. Hoon, M. *et al.* Neuroligin-4 is localized to glycinergic postsynapses and regulates inhibition in the retina. *Proc. Natl. Acad. Sci. U. S. A.* **108**, 3053–3058 (2011).
11. Rinaldi, T., Silberberg, G. & Markram, H. Hyperconnectivity of Local Neocortical Microcircuitry Induced by Prenatal Exposure to Valproic Acid. *Cereb. Cortex* **18**, 763–770 (2008).
12. Turrigiano, G. G., Leslie, K. R., Desai, N. S., Rutherford, L. C. & Nelson, S. B. Activity-dependent scaling of quantal amplitude in neocortical neurons. *Nature* **391**, 892–896 (1998).
13. Le Bé, J.-V. & Markram, H. Spontaneous and evoked synaptic rewiring in the neonatal neocortex. *Proc. Natl. Acad. Sci. U. S. A.* **103**, 13214–13219 (2006).
14. Rinaldi, T., Kulangara, K., Antoniello, K. & Markram, H. Elevated NMDA receptor levels and enhanced postsynaptic long-term potentiation induced by prenatal exposure to valproic acid. *Proc. Natl. Acad. Sci. U. S. A.* **104**, 13501–13506 (2007).
15. Budreck, E. C. & Scheiffele, P. Neuroligin-3 is a neuronal adhesion protein at GABAergic and glutamatergic synapses. *Eur. J. Neurosci.* **26**, 1738–1748 (2007).
16. Bolliger, M. F. *et al.* Unusually rapid evolution of Neuroligin-4 in mice. *Proc. Natl. Acad. Sci.* **105**, 6421–6426 (2008).
17. Jamain, S. *et al.* Mutations of the X-linked genes encoding neuroligins NLGN3 and NLGN4 are associated with autism. *Nat. Genet.* **34**, 27–29 (2003).
18. Tsodyks, M., Pawelzik, K. & Markram, H. Neural networks with dynamic synapses. *Neural Comput.* **10**, 821–835 (1998).
19. House, D. R. C., Elstrott, J., Koh, E., Chung, J. & Feldman, D. E. Parallel regulation of feedforward inhibition and excitation during whisker map plasticity. *Neuron* **72**, 819–831 (2011).
20. Larkum, M. E., Kaiser, K. M. M. & Sakmann, B. Calcium electrogenesis in distal apical dendrites of layer 5 pyramidal cells at a critical frequency of back-propagating action potentials. *Proc. Natl. Acad. Sci.* **96**, 14600–14604 (1999).
21. Missler, M. *et al.* α-Neurexins couple Ca2+ channels to synaptic vesicle exocytosis. *Nature* **423**, 939–948 (2003).
22. Le Bé, J.-V. & Markram, H. Spontaneous and evoked synaptic rewiring in the neonatal neocortex. *Proc. Natl. Acad. Sci. U. S. A.* **103**, 13214–13219 (2006).
23. Lüthi, A., Laurent, J.-P., Figurovt, A., Mullert, D. & Schachnert, M. Hippocampal long-term potentiation and neural cell adhesion molecules L1 and NCAM. Publ. Online 29 Dec. 1994 Doi101038372777a0 **372**, 777–779 (1994).
24. Muller, D. *et al.* PSA-NCAM is required for activity-induced synaptic plasticity. *Neuron* **17**, 413–422 (1996).
25. Laumonnier, F. *et al.* X-linked mental retardation and autism are associated with a mutation in the NLGN4 gene, a member of the neuroligin family. *Am. J. Hum. Genet.* **74**, 552–557 (2004).
26. Chih, B., Afridi, S. K., Clark, L. & Scheiffele, P. Disorder-associated mutations lead to functional inactivation of neuroligins. *Hum. Mol. Genet.* **13**, 1471–1477 (2004).
27. Gogolla, N. *et al.* Common circuit defect of excitatory-inhibitory balance in mouse models of autism. *J. Neurodev. Disord.* **1**, 172–181 (2009).
28. Rubenstein, J. L. R. & Merzenich, M. M. Model of autism: increased ratio of excitation/inhibition in key neural systems. *Genes Brain Behav.* **2**, 255–267 (2003).
29. Polleux, F. & Lauder, J. M. Toward a developmental neurobiology of autism. *Ment. Retard. Dev. Disabil. Res. Rev.* **10**, 303–317 (2004).
30. Lin, H.-C., Gean, P.-W., Wang, C.-C., Chan, Y.-H. & Chen, P. S. The amygdala excitatory/inhibitory balance in a valproate-induced rat autism model. *PloS One* **8**, e55248 (2013).
31. Markram, H., Rinaldi, T. & Markram, K. The intense world syndrome - an alternative hypothesis for autism. *Front. Neurosci.* **1**, 77–96 (2007).
32. Monyer, H. *et al.* Heteromeric NMDA receptors: molecular and functional distinction of subtypes. *Science* **256**, 1217–1221 (1992).
33. Tabuchi, K. *et al.* A neuroligin-3 mutation implicated in autism increases inhibitory synaptic transmission in mice. *Science* **318**, 71–76 (2007).
34. Karim, F., Wang, C. C. & Gereau, R. W., 4th. Metabotropic glutamate receptor subtypes 1 and 5 are activators of extracellular signal-regulated kinase signaling required for inflammatory pain in mice. *J. Neurosci. Off. J. Soc. Neurosci.* **21**, 3771–3779 (2001).
35. Pillai-Nair, N. *et al.* Neural cell adhesion molecule-secreting transgenic mice display abnormalities in GABAergic interneurons and alterations in behavior. *J. Neurosci. Off. J. Soc. Neurosci.* **25**, 4659–4671 (2005).
36. Bouzioukh, F., Tell, F., Jean, A. & Rougon, G. NMDA receptor and nitric oxide synthase activation regulate polysialylated neural cell adhesion molecule expression in adult brainstem synapses. *J. Neurosci. Off. J. Soc. Neurosci.* **21**, 4721–4730 (2001).
37. Bloom, O. *et al.* Colocalization of synapsin and actin during synaptic vesicle recycling. *J. Cell Biol.* **161**, 737–747 (2003).

Acknowledgements

We would like to thank N. Brose, O. Hagens, M. Telefont, M. Pezzoli and S. Muralidhar for comments and helpful discussions. This work was supported by the EPFL and Asterion Foundation.

Author contributions

The authors declare that the research was conducted in the absence of any commercial or financial relationships that could be construed as a potential conflict of interest. Electrophysiological experiments were conducted by V.D.; Western Blots were done by D.L.M.; J.M. handled the mice colony and animals genotyping. This manuscript has been written by V.D., H.M. and K.M.

Additional information

Supplementary information accompanies this paper at http://www.nature.com/scientificreports

Competing financial interests: The authors declare that the research was conducted in the absence of any commercial or financial relationships that could be construed as a potential conflict of interest.

How to cite this article: Delattre, V., La Mendola, D., Meystre, J., Markram, H. & Markram, K. *Nlgn4* knockout induces network hypo-excitability in juvenile mouse somatosensory cortex *in vitro*. *Sci. Rep.* **3**, 2897; DOI:10.1038/srep02897 (2013).